RASĀYAN *J. Chem.*
Vol. 19 | No. 4 | 2030-2036 | October-December | 2026
ISSN: 0974-1496 | e-ISSN: 0976-0083 | CODEN: RJCABP
http://www.rasayanjournal.com
http://www.rasayanjournal.co.in

HOLMIUM DOPED ZINC MOLYBDATE: AN EFFICIENT PHOTO CATALYST FOR DYE DEGRADATION

B. Kande[1], R. K. Sahu[2], B. Jain[3], and P. P. Nimje[1,✉]
[1]Department of Chemistry, Shri Shankaracharya Professional University, Bhilai, Chhattisgarh, India
[2]Department of Chemistry, Govt. Engineering College Ambikapur, Chhattisgarh, India
[3]Department of Chemical Sciences, Siddhachalam Laboratory, Raipur, Chhattisgarh, India
✉Corresponding author: prachinimje56@gmail.com

ABSTRACT
The nano material based on holmium-doped zinc molybdate has proven to have considerable antibacterial and photocatalytic capabilities. The zinc molybdate doped with holmium (Ho-$ZnMoO_4$) was synthesized and its properties were characterized by different techniques such as UV spectroscopy, Fourier-transform infrared spectroscopy (FTIR), X-ray diffraction (XRD), scanning electron microscopy (SEM) and field-emission scanning electron microscopy (FESEM). UV spectroscopy analysis indicated the optical characteristics of Ho-$ZnMoO_4$, giving insights into its absorption and electronic transitions. The synthesized material was analysed for the presence of functional groups by FTIR spectroscopy. The XRD analysis was useful to examine the crystal structure and phase purity of Ho-$ZnMoO_4$. The surface morphology and microstructure of the synthesized material were obtained in detail from the SEM and FESEM images. Additionally, the paper investigated the photocatalytic properties of Ho-$ZnMoO_4$. The synthesis of the Ho-doped $ZnMoO_4$ and its photo-catalysis properties was successfully performed in this study.
Keywords: Holmium-Doped Zinc Molybdate, Photocatalytic Properties, UV Spectroscopy, X-Ray Diffraction.
RASĀYAN *J. Chem.*, Vol. 19, No.4, 2026

INTRODUCTION

Nanostructured metal oxides captured their interest in recent decades due to their distinctive prospective applications.[1] These nanomaterials, which were made up of tiny particles and regularly changed their important physical and chemical properties, had the ability to expand and establish themselves as entirely new phenomena.[2] On the other hand, properties and uses of tungstates (MWO_4) and molybdates ($MMoO_4$), were quite interesting, like catalysis, photocatalysis, and luminescence etc.[3-4] Nanostructured metal oxides such as tungsten and molybdates exhibit significant photocatalytic properties due to their controlled textural and morphological features, variable surface chemistry, and broad specific surface areas.[5] These materials, when in nanostructured form, demonstrate novel functionalities arising from quantum size effects and confinement, making them attractive for various applications, including photocatalysis.[6] The utilization of efficient solar energy for environmental remediation is a key challenge, with transition metal oxide nanoparticles playing a crucial role in facilitating photocatalytic applications under visible light.[7] Additionally, the synthesis of visible light active nano-sized photocatalysts using metal oxides like tungsten oxide and molybdates has shown promising results in inhibiting the growth of harmful algal blooms, showcasing their potential for biological applications.[8] Rare earth metal cations, including elements like Yttrium (Y), Dysprosium (Dy), Terbium (Tb), and Gadolinium (Gd), exhibit diverse coordination chemistry and magnetic properties.[9] These cations are crucial components in the synthesis of coordination compounds with unique structures, such as bimetallic borohydride-bridged compounds and rare earth mixed ligand complexes.[10] Rare earth elements, which encompass Sc, Y, and the lanthanide series, are utilised in various fields due to their exceptional electronic, optical, and magnetic characteristics.[11] Additionally, the adsorption competencies of rare earth metal cations in materials like γ-zirconium phosphate have been studied, showcasing their distinct behaviour based on ionic radius. Overall, rare earth metal cations play vital roles in the development of advanced materials with applications ranging from photovoltaics to catalysis. Rare earth metal cations, emission spectra

http://doi.org/10.31788/RJC.2026.1939732

should be dominated by 4f-4f or 4f-5d electronic transitions. The band gap between stimulated energy levels and ground energy levels determines their emission wavelength.[12] The Mo^{6+} cation in molybdates $(MoO_4)^{2-}$ had a core metal ion surrounded by four O^{2-} anions, with tetrahedral coordination, and it made up a stable component structure.[13] Some rare earth cations activated molybdate substances, including $CaMoO_4$, $BaMoO_4$, $SrMoO_4$, $ZnMoO_4$, and $MgMoO_4$.[14-15] Second metal ions, including Li^+, Mg^+, and K^+ were injected to increase the luminescent characteristics of those materials to boost activity.[16] Holmium was selected among rare earth elements due to its unique 4f electronic configuration and ionic radius, which we hypothesised would effectively modify the band structure of zinc molybdate. Previous studies have shown holmium's potential in improving photocatalytic activity in other materials (cite relevant studies). While the rare earth doping approach is established, our study uniquely applies this to zinc molybdate, addressing a gap in the literature regarding holmium's effects on this specific material. Here, the synthesised Holmium-doped Zinc molybdate ($HoZnMoO_4$) nano material. And also characterised it by UV-visible spectroscopy, band gap energy analysis, FTIR spectroscopy, X-ray diffraction (XRD), scanning electron microscope (FESEM) and weight percentage of element determined via EDS. And also explore the biological and photocatalytic application of Holmium-doped zinc molybdate nano materials.

EXPERIMETNAL

Materials

The analytical-grade reagents used for the synthesis were zinc sulphate heptahydrate (99.8%, Merck), sodium molybdate dihydrate (99.8%, Merck) and holmium nitrate hexahydrate ($Ho(NO_3)_3 \cdot 6H_2O$, 99.99% purity). Other chemicals used, including acetone, ethylene glycol (Merck), urea (HiMedia) and methylene blue dye (S.D. Fine Chemicals), were used without modification. Commercial sources of all reagents were used without any special purification treatment. All the experimental investigations were carried out with triple-distilled water prepared in an all-glass distillation assembly to exclude any contamination caused by metallic impurities.

Synthesis of Holmium Doped Zinc Molybdate ($HoZnMoO_4$)

A beaker of 1 M $ZnSO_4 \cdot 7H_2O$ solution was prepared, and 10 mL of ethylene glycol was added to it and stirred continuously, followed by the addition of 2M $Na_2MoO_4 \cdot 2H_2O$ solution to the prepared solution with continuous stirring. The pH of the reaction mixture was adjusted to 9.0 with urea and then heated at 80°C for 1 hour. Then, 1 g of $Ho(NO)_3 \cdot 6H_2O$ was added to the solution and transferred to a round-bottom flask and kept under continuous stirring at 120°C.[4] The suspension was left to settle down after completion of the reaction, and the solution was filtered out after complete settlement of the precipitate. The precipitate obtained was washed with deionised water, methanol and acetone for the removal of the impurities. It was initially dried at 60°C for 2h, then calcined at 550°C to get the final crystalline material.[11] Synthesized compound was also used in the antibacterial test against Gram-positive and Gram-negative bacterial strains, and it was also used in removing the methylene blue dye from water.[19]

Characterization

The synthesized material was characterized by its crystalline features by recording its UV–Visible absorption spectra in absorbance mode (samples dispersed in ethanol) using a UV-1900i double-beam spectrophotometer and also using an Advanced D8 Bruker X-ray diffractometer with Ni-filtered Cu-Kα radiation (λ = 1.5405 Å) in the range of 2θ of 10–80° with a step size of 0.02°.[12] Surface morphology and microstructural features were analysed by the CARL ZEISS UHR FESEM, Model GEMINI SEM 500 KMAT under 0.8 nm resolution and probe current in the range 3pA – 100nA.[22] Fourier transform infrared (FT-IR) spectra were obtained using an Avtar 370 Thermo Nicolet spectrophotometer with a resolution of 4 cm^{-1}, and the samples were prepared in the form of KBr pellets for spectral measurement.[17-18]

Dye Remediation

For the photocatalytic experiment, methylene blue (MB) dye was used as a model organic pollutant in the presence of the synthesised nanomaterial. A stock solution of methylene blue was prepared and then diluted with deionised water to the desired concentration. The synthesized $ZnMoO_4$ composite nanomaterials were transferred to a flask containing a fixed volume of dye solution (10 mL, 5 ppm) and

the reaction mixture was then subjected to sonication for 120 min at pH 6 for ambient temperature. After a fixed time, the reaction mixture was permitted to equilibrate, and the absorbance was measured at 600 nm on a UV–Visible spectrophotometer (UV-1900i, Shimadzu, Japan). After the experiment, the nanocomposites were separated from the reaction medium by centrifugation, and the removal efficiency (R, %) of methylene blue dye was calculated by using eqn.-i.

$$R\ (\%) = \frac{Co - Ce}{Co} \times 100 \qquad \text{(i)}$$

Where,
C_o = initial concentration of methylene blue (mg L^{-1});
C_e = equilibrium concentration of methylene blue (mg L^{-1}).

RESULTS AND DISCUSSION

Characterization

UV-Vis Absorption

The optical properties of the synthesised holmium-doped zinc molybdate nanoparticles (Fig.-1) were studied using UV–Visible spectroscopy. The absorption peak of the UV spectrum was very clearly visible at about 270 nm, and the Tauc plot of $HoZnMoO_4$ showed a band gap energy of 2.6 eV. The results obtained showed noticeable differences in optical properties and functional performance. The $HoZnMoO_4$ nanoparticles had a lower band gap value (2.6 eV) compared to pristine $ZnMoO_4$ (3.2 eV), and this was attributed to the enhanced absorption in the visible light region.[21]

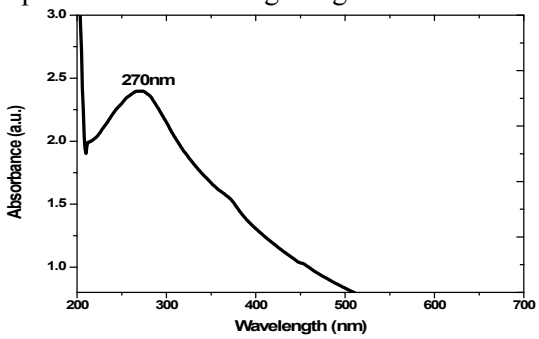

Fig.-1: UV−Vis Absorption Spectrum of Ho-doped $ZnMoO_4$ Nano Material

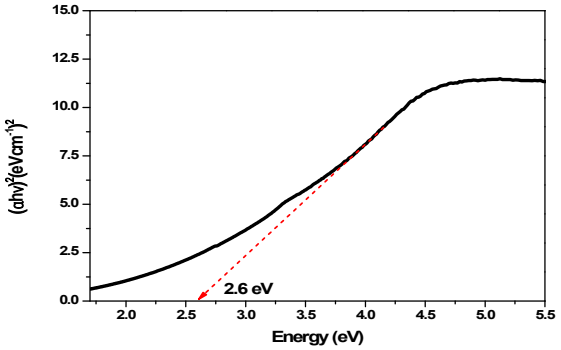

Fig.-2: Tauc Plot of Ho-doped $ZnMoO_4$, which was derived from UV-Vis Absorption. Where the Band Gap Value (E_g) was 2.6 eV

Fourier Transformed Infrared Spectra

FTIR spectroscopy was used to determine the chemical structure and functional groups of $HoZnMoO_4$. The FTIR spectrum obtained between 500 and 4000 cm^{-1} is given in Fig.-3. A few characteristic bands were seen: the peaks at 3440.7 and 1633.8 cm^{-1} were due to the O–H stretching and bending vibrations of the absorbed water molecules, or H–O–H groups.17 The bands at 1180.2 and 1105.7 cm^{-1} were assigned to the $[MoO_\gamma]^{n-}$ groups, and the peak at 825.6 cm^{-1} to Zn–O stretching vibrations in Zn molybdate.[18,19]

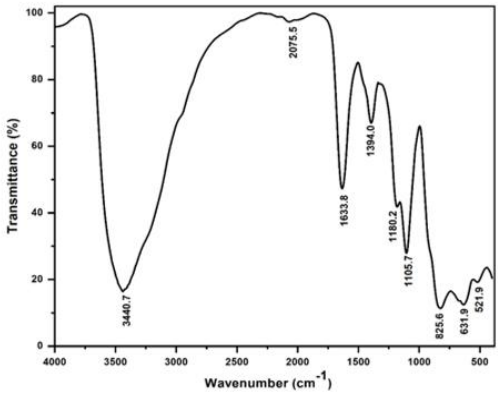

Fig.-3: FTIR Spectrum of $HoZnMoO_4$ Nano Material

The band observed at 2075.5 cm^{-1} was assigned to a minor amount of organic contamination formed during the sample preparation process. The FTIR spectrum of $HoZnMoO_4$ was found to be similar to that of pure $ZnMoO_4$, suggesting the incorporation of Ho in the host lattice was successful. Other characteristic peaks at 631.9, 521.9 and 1394.0 cm^{-1} were attributed to the Zn–O and Ho–Zn vibrations in the $HoZnMoO_4$ nanomaterial, however.[20]

X-ray Diffraction (XRD)

The diffraction peaks found in all samples were found to be in agreement with the hexagonal phase formation of $HoZnMoO_4$. The structural properties of the synthesized zinc molybdate nanomaterial were investigated using X-ray diffraction (XRD), and the obtained pattern indicated its crystalline nature, as illustrated in Fig.-4.[9] The prominent diffraction peaks observed at 2θ values of 14.2°, 19.1°, 20°, 25.2°, 28.7°, 30.9°, 34.2°, 35.9°, 39.2°, 41.2°, 49.8°, 54.6°, 59.1°, and 65° corresponded to the crystallographic planes (001), (110), (020), (120), (022), (221), (222), (132), (040), (330), (122), (111), and (110), respectively.[14] In addition, the diffraction peak related to the (221) plane suggested the synergistic effect of Ho/Zn oxide in the crystal lattice structure. The crystallite size, calculated by the Debye–Scherrer equation, was found to be 65.7 nm.[23]

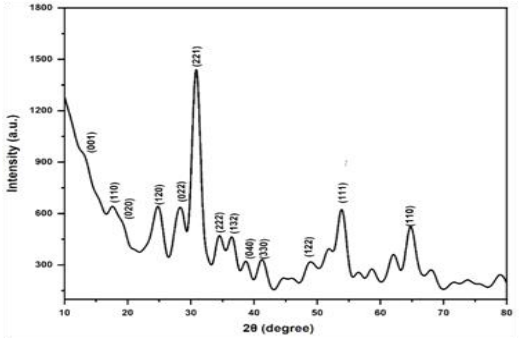

Fig.-4: X-ray Diffraction Spectrum of Holmium Zinc Molybdate ($HoZnMoO_4$) Nano Material

Field Emission Scanning Electron Microscopy (FESEM) & Energy Dispersive Spectroscopy (EDS)

As seen in Fig.-5a, the disc-shaped hexagonal morphology of the $HoZnMoO_4$ nanomaterial showed aggregation due to the presence of binary holmium and zinc oxides. Both the fact that the composite was in crystalline form and the presence of holmium embedded on the $ZnMoO_4$ surface, which produced a unique nanomaterial, were persuasively shown. The elemental composition and purity of the Ho-doped $ZnMoO_4$ nanomaterial were evaluated by EDS analysis (Fig.-5bc). EDS spectra and mapping reveal uniform distribution of Ho, Zn, Mo, C, and O throughout the entire matrix (Fig.-5b & c). No more matching impurity peaks was discovered. Its smooth surface was associated with the single-phase surface morphology observed due to the heterogeneous mixing of Ho, Zn, and Mo oxides (Fig.-5).

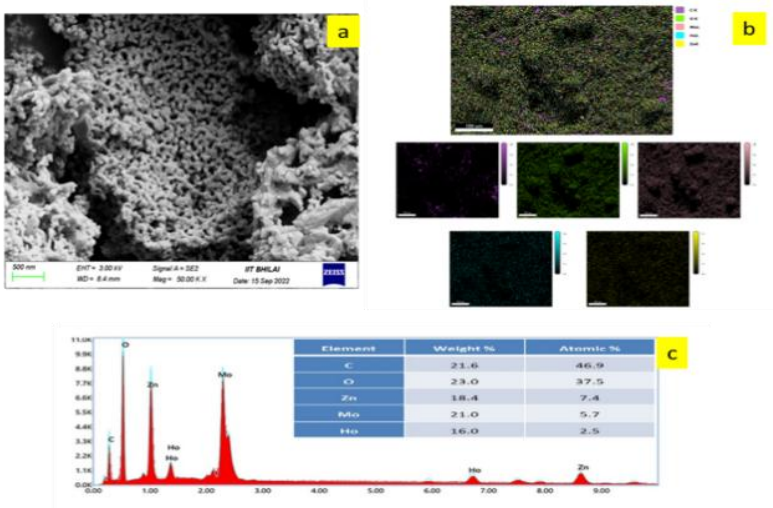

Fig.-5: (a)FESEM Image of Ho-Doped $ZnMoO_4$ Nano Material, (b) EDS Mapping for Ho Doped $ZnMoO_4$ Nano Material, (c) EDS Spectrum of Ho-doped $ZnMoO_4$ Nano Material with Inset Table of Weight Percentage

Photocatalysis

We discussed the photocatalysis reaction of ZnMoO4 nanomaterial doped with Ho during the photodegradation process using methylene blue. 40.0 mg of HoZnMoO4 nanomaterial in air and light. added to a 10.0 ml aqueous methylene blue (1.0 x 10-4 M) solution (pH = 6). Ho-ZnMoO4 nanomaterial reduced the blue colour of the solution at regular intervals of 10 minutes (Fig.-6). The methylene blue aqueous solution was scanned between 200 and 700 nm, with a λmax of 578 nm

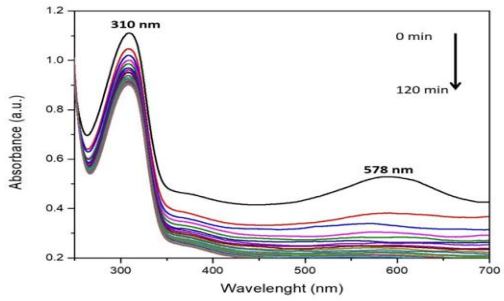

Fig.-6: Photo-catalytic Reaction of Ho Doped $ZnMoO_4$(Ho-$ZnMoO_4$) Nano Material. (40.0 mg) via Methylene Blue (1.0×10^{-4} M) Degradation in Presence of Light and Air at 578 nm Wavelength

Mechanism

Ho-doped $ZnMoO_4$ nanomaterial photodegradation starts with light absorption, which produces O_2 and OH radicals as well as electron-hole pairs when exposed to visible light. These extremely potent radicals reduce the production of non-toxic byproducts (CO_2 and H_2O) and initiate breakdown in aqueous solution. Highly active sites on large surfaces enhanced the maximum interactions between the Ho-doped $ZnMoO_4$ nanomaterial and the methylene blue dye. Superoxide anion radicals ($*O^{2-}$) and $*OH^-$ radicals are produced when the interaction between OH^- and holes begins. H_2O molecules were changed into OH as the electrons interacted with the Nanocatalyst. The radicals produced in the reaction ($*O^{2-}$ and $*OH^-$), This is extremely reactive for the breakdown of methylene blue and produces CO_2 and H_2O, two non-toxic byproducts. The following is the mechanism of photo-degradation:

$$\text{Ho-ZnMoO}_4 + h\upsilon \rightarrow \text{Ho-ZnMoO}_4^* + e^- + h^+$$

$$e^- + O_2 \rightarrow *O_2^-$$

$$h^+ + H_2O \rightarrow *OH^-$$

$$MB + *OH^- \rightarrow CO_2 + H_2O \text{ (by-product)}$$

$$MB + *O_2^- \rightarrow CO_2 + H_2O \text{ (by-product)}$$

The photodegradation of an aqueous solution of methylene blue dye in the presence of light and air demonstrated the photocatalytic activities of the zinc molybdate nanomaterial doped with holmium.

CONCLUSION

Holmium-doped zinc molybdate nanomaterial was created using the co-precipitation method, in which water was used as a solvent. The reaction between the two species in the presence of water produced hydroxyl ions for precipitation, resulting in a hexagonal crystalline structure that was detected by XRD. The morphology was observed using FESEM; all images demonstrated the presence of zinc molybdate on the surface of Holmium, forming $HoZnMoO_4$ nano material, which was characterised using UV-visible spectroscopy, FTIR spectroscopy, and X-ray diffraction (XRD). In the presence of water, the two species' interaction produced hydroxyl ions that precipitated. XRD revealed a solid with a hexagonal crystalline structure. The morphology was examined using a FESEM; every image revealed the formation of $HoZnMoO_4$ nanomaterial and the presence of zinc molybdate on the surface of holmium. X-ray diffraction (XRD), FTIR spectroscopy, band gap energy measurement, and UV-visible spectroscopy were used to investigate this nanomaterial. The elemental composition and purity of the Ho-doped $ZnMoO_4$ nanomaterial were evaluated by EDS analysis. Additionally, it demonstrated an impressive photocatalytic ability with methylene blue. When methylene blue was degraded at pH 6, Ho-$ZnMoO_4$ demonstrated good catalytic efficiency. Methylene blue loses its blue hue over a consistent period of time. The colour of the solution changed from blue to colourless after 120 minutes. The entire process made it simple to extract the catalyst through separation and centrifugation.

ACKNOWLEDGEMENTS

We are very thankful to SAIF Kochi for providing analysis facilities.

CONFLICT OF INTEREST

Authors declares no conflict of interest.

AUTHOR CONTRIBUTIONS

The present work is related to *SDG-6: Clean Water and Sanitation*. All the authors contributed significantly to this manuscript, participated in reviewing/editing and approved the final draft for publication. The research profile of the authors can be verified from their ORCID ids, given below:

Bhupendra Kande https://orcid.org/0009-0008-5917-0027
Rajesh Kumar Sahu https://orcid.org/0009-0008-8184-6193
Bhawana Jain https://orcid.org/0000-0003-0272-3344
Prachi P. Nimje https://orcid.org/0009-0000-4655-8972

Cite this article as: B. Kande *et al.*, *Rasayan J. Chem.*, 19(4), 2030-2036(2026), https://doi.org/10.31788/RJC.2026.1949732

REFERENCES

1. F. Nastase, I. Stamatin, C. Nastase, D. Mihaiescu, and A. Moldovan, *Progress in Solid State Chemistry*, **34**, 191(2006), https://doi.org/10.1016/j.progsolidstchem.2005.11.022
2. B. Jain, A. Hashmi, S. Sanwaria, A. K. Singh, Md. A. B. H. Susan, and A. Singh, *Advanced Composites and Hybrid Materials*, **3**, 231(2020), https://doi.org/10.1007/s42114-020-00153-5
3. V. D. Zhuravlev, O. G. Reznitskikh, Yu. A. Velikodnyi, T. A. Patrusheva, and O. V. Sivtsova, *Journal of Solid State Chemistry,* **184,** 2785(2011), https://doi.org/10.1016/j.jssc.2011.08.003
4. J. Ungelenk, M. Speldrich, R. Dronskowski, and C. Feldmann, *Solid State Sciences*, **31**, 62(2014), https://doi.org/10.1016/j.solidstatesciences.2014.02.020
5. M. Ikram, U. Qumar, S. Ali, and A. Ul-Hamid, in *Advanced Materials for Wastewater Treatment and Desalination*, CRC Press, 53(2022), https://doi.org/10.1201/9781003167327-4

6. S. Surnev and F. P. Netzer, *Journal of Physics: Condensed Matter*, **34**, 233001(2022), https://doi.org10.1088/1361-648X/ac4ceb
7. J. Patel, B. Jain, A. K. Singh, M. A. B. H. Susan, and L. Jean-Paul, *Microchemical Journal*, **155**, 104755(2020), https://doi.org/10.1016/j.microc.2020.104755
8. A. Moharana, A. Kumar, A. Thakur, D.V. N. Vo, A. Sharma, and D. Kumar, in *Nanostructured Photocatalysts*, 145(2021), https://doi.org/10.1016/B978-0-12-823007-7.00010-9
9. C. G. T. Price, A. Mondal, J. P. Durrant, J. Tang, and R. A. Layfield, *Inorganic Chemistry*, 9924(2023), https://doi.org/10.1021/acs.inorgchem.3c01038
10. L. Zeybel and D. A. KÖSE, *Turkish Journal of Chemistry***,** **45**, 1004(2021), https://doi.org/10.3906/kim-2012-47
11. T. Takei, K. Iidzuka, A. Miura, S. Yanagida, N. Kumada, E. Magome, C. Moriyoshi and Y. Kuroiwa, *Langmuir*, **32,** 9993(2016), https://doi.org/10.1021/acs.langmuir.6b02747
12. D.A. Spassky, A.N. Vasil'Ev, I.A. Kamenskikh, V.V. Mikhailin, A.E. Savon, Yu. A. Hizhnyi, S.G. Nedilko, and P.A. Lykov, *Journal of Physics: Condensed Matter*, **23**, 365501(2011), https://doi.org/10.1088/0953-8984/23/36/365501
13. L.Y. Zhou, J. S. Wei, F.Z. Gong, J.L. Huang, and L.H. Yi, *Journal Solid State Chemistry*, **181**, 1337(2008), https://doi.org/10.1016/j.jssc.2008.03.005
14. M.J. Kim and Y.D. Huh, *Optical Materials*, **35**, 263(2012), https://doi.org/10.1016/j.optmat.2012.08.012
15. D. Hu, W. Huan, Y. Wang, and Y. Wang, *Journal of Materials Science: Materials in Electronics***, 26,** 7290(2015), https://doi.org/10.1007/s10854-015-3356-x
16. C. L. Han, L. Luo, J. Q. He, J. X. Wang, and W. Zhang, *Journal of Materials Science: Materials in Electronics***, 28**, 4409(2017), https://doi.org/10.1007/s10854-016-6069-x
17. R. L. Frost and S. J. Palmer, *Journal of Raman Spectroscopy*, **42**, 2042(2011), https://doi.org/10.1002/jrs.2959
18. C. Pholnak, C. Sirisathitkul, and D. J. Harding, *Journal of Physics and Chemistry of Solids***, 72,** 817(2011), https://doi.org/10.1016/j.jpcs.2011.04.005
19. S. Pataila, A. K. Singh, B. Jain, and G. S. Thool, *Asian Journal of Chemistry*, **29**, 2409(2017), https://doi.org/10.14233/ajchem.2017.20704
20. H. Oudghiri-Hassani, S, Rakass, M. Abboudi, A. Mohmoud, F. Al Wadaani, *Molecules,* **23,** 1462 (2018) https://doi.org/10.3390/molecules23061462
21. A. P. de Azevedo Marques *et al*, *J0urnal of Solid State Chemistry*, **179,** 671(2006), https://doi.org/10.1016/j.jssc.2005.11.020
22. J. H. Ryu, J.-W. Yoon, C. S. Lim, W.-C. Oh, and K. B. Shim, *Journal of Alloys and Compounds***, 390,** 245(2005), https://doi.org/10.1016/j.jallcom.2004.07.064
23. A. M. Edwin Suresh Raj, C. Mallika, K. Swaminathan, O. M. Sreedharan, and K. S. Nagaraja, *Sensors and Actuators B: Chemical***, 81,** 229(2002), https://doi.org/10.1016/S0925-4005(01)00957-1

[RJC-9732/2026]